

Published in final edited form as:

*Gastroenterology*. 2010 September ; 139(3): 918–928.e6. doi:10.1053/j.gastro.2010.05.081.

## Atonal homolog 1 is required for growth and differentiation effects of Notch/ $\gamma$ -secretase inhibitors on normal and cancerous intestinal epithelial cells

Avedis Kazanjian<sup>1</sup>, Taeko Noah<sup>1</sup>, Douglas Brown<sup>4</sup>, Jarred Burkart<sup>3</sup>, and Noah F. Shroyer<sup>1,2,4</sup>

<sup>1</sup>Cincinnati Children's Hospital Medical Center, Division of Gastroenterology, Hepatology, and Nutrition

<sup>2</sup>Cincinnati Children's Hospital Medical Center, Division Developmental Biology

<sup>3</sup>Cincinnati Children's Hospital Medical Center, Summer Undergraduate Research Fellowship program

<sup>4</sup>University of Cincinnati, College of Medicine

### Abstract

**Background & Aims**—The Atonal Homolog 1 (Atoh1 or Math1) transcription factor is required for intestinal secretory (goblet, Paneth, enteroendocrine) cell differentiation. Notch/ $\gamma$ -secretase inhibitors (GSIs) block proliferation and induce secretory cell differentiation in the intestine. We used genetic analyses of mice to determine whether Atoh1 mediates the effects of GSIs in normal and cancerous intestinal epithelia.

**Methods**—We studied mice with intestine-specific disruption of *Atoh1* (*Atoh1* <sup>$\Delta$ intestine</sup>), the *APC*<sup>min</sup> mutation, both mutations [*Atoh1* <sup>$\Delta$ intestine</sup>; *APC*<sup>min</sup>], or littermate controls; mice were given GSI or vehicle. Colorectal cancer (CRC) cell lines were treated with GSI or vehicle and with small hairpin (sh) RNAs to reduce *ATOH1*. Differentiation and homeostasis was assessed by protein, RNA, and histologic analyses.

**Results**—GSIs failed to induce secretory cell differentiation or apoptosis or decrease proliferation of *Atoh1*-null progenitor cells, compared with wild-type cells. Exposure of *APC*<sup>min</sup> adenomas to GSIs decreased proliferation and increased secretory cell numbers in an Atoh1-dependent manner. In CRC cells treated with GSI, ATOH1 levels were inversely correlated with proliferation. ATOH1 was required for secretory cell gene expression in cell lines and in mice.

**Conclusions**—ATOH1 is required for all effects of GSIs in intestinal crypts and adenomas; Notch has no unique function in intestinal progenitors and cancer cells other than to regulate

© 2010 The American Gastroenterological Association. Published by Elsevier Inc. All rights reserved

Address correspondence to: Noah F. Shroyer, Ph.D., Division of Gastroenterology, Hepatology, and Nutrition, Cincinnati Children's Hospital, MLC 2010, 3333 Burnet Ave, Cincinnati OH 45229, noah.shroyer@cchmc.org, Office: (513) 636-0129, Laboratory: (513) 636-7082, Fax: (513) 636-5581.

The authors have no disclosures to report.

Author contributions: AK, NFS conceived and designed the experiments  
AK, TN, DB, JB, NFS performed and interpreted the experiments  
AK and NFS wrote the manuscript.

**Publisher's Disclaimer:** This is a PDF file of an unedited manuscript that has been accepted for publication. As a service to our customers we are providing this early version of the manuscript. The manuscript will undergo copyediting, typesetting, and review of the resulting proof before it is published in its final citable form. Please note that during the production process errors may be discovered which could affect the content, and all legal disclaimers that apply to the journal pertain.

ATOH1 expression. Reducing ATOH1 activity might mitigate intestinal toxicity from systemic GSI therapy for non-intestinal diseases. Among gastrointestinal malignancies, ATOH1 mediates the effects of GSIs, so ATOH1 expression levels might predict responses to these inhibitors. We propose that only the subset of CRCs that retain ATOH1 expression will respond to GSIs.

### Keywords

biomarkers; cell fate specification; basic helix-loop-helix transcription factor; notch intracellular domain

---

Molecular pathways that regulate normal development and homeostasis are frequently misregulated in cancers and represent potential targets for clinical intervention. The Notch signaling pathway is key to determining self-renewal versus differentiation of intestinal stem cells. The importance of Notch signaling in colorectal cancer (CRC) tumorigenesis has only recently been recognized, suggesting that this pathway is a target for new CRC therapeutics<sup>1</sup>.

The intestinal epithelium is composed of three main cell types: “absorptive” enterocytes, and three “secretory” cell types: Paneth, enteroendocrine, and goblet cells. Notch signaling controls the fate of intestinal progenitors by differentially regulating two opposing basic helix-loop-helix (bHLH) transcription factors, *HAIRY/ENHANCER OF SPLIT 1* (*HES1*, also called *HRY*)<sup>2</sup> and *ATONAL HOMOLOG 1* (*ATOH1*, also called *Math1* or *HATH1*)<sup>3</sup>. Progenitors with low levels of Notch express high levels of *ATOH1* and commit to a secretory cell fate, whereas progenitors with high levels of active Notch express *HES1*, which in turn repress *ATOH1*, and become absorptive enterocytes<sup>1, 4–9</sup>. This model of alternate fate selection is based upon regulation of *Notch*, *atonal*, and *enhancer-of-split* genes via lateral inhibition in *Drosophila melanogaster*<sup>10–11</sup>. Thus, ATOH1 is thought to be a critical gatekeeper for the program of Notch-directed differentiation of intestinal stem cells.

Recent studies report loss of *ATOH1* expression in human CRCs<sup>12</sup>. We recently confirmed that ~80% of human CRCs silence *ATOH1*, and showed that the mechanism includes both genetic and epigenetic silencing<sup>13</sup>. Moreover, we showed that *Atoh1* mutant mice (*Atoh1*<sup>*Δintestine*</sup>) are highly susceptible to tumor formation using both azoxymethane and *APC*<sup>*min/+*</sup> mouse models of CRC<sup>13</sup>. Taken together, these results suggest that *ATOH1* may be the key target of the Notch pathway regulating differentiation and proliferation within CRCs.

$\gamma$ -secretase inhibitors (GSIs) are small molecules first developed for their ability to inhibit processing of the Alzheimer’s related  $\beta$ -amyloid peptide (A $\beta$ ) from the amyloid precursor protein (APP)<sup>14</sup>. Subsequently, these drugs were shown to also inhibit ligand-dependent Notch cleavage and activation<sup>15</sup>. More recently, Notch-sparing GSIs have been developed that selectively inhibit APP processing but have less effect on Notch processing, and thus avoid potential side effects on Notch-regulated organ systems such as the intestine<sup>16</sup>. In contrast, nonselective GSIs cause a dose-dependent conversion of small intestinal and colonic progenitors to the secretory cell fate, accompanied by activation of *Atoh1* and downregulation of *Hes1* expression in intestinal crypt progenitors<sup>1, 17–19</sup>. Additionally, treatment of *APC*<sup>*min/+*</sup> mice with GSIs resulted in reduced proliferation, *Atoh1* overexpression, and differentiation of some adenoma cells to nonproliferating goblet cells<sup>1</sup>. More recently, GSI treatment was shown to quantitatively shrink adenomas in *APC*<sup>*min/+*</sup> mice<sup>20</sup>. Experiments in CRC cell lines showed a minimal effect of GSI alone, but a pro-apoptotic effect when given in combination with cytotoxic drugs such as taxanes or platinum compounds<sup>21–23</sup>. In addition to these effects, GSIs have been proposed as chemotherapeutic

agents in Barrett's esophagus, gastric cancer, and several non-GI cancers<sup>23–25</sup>. Thus, Notch-targeted GSI is a promising class of small molecules for treatment of gastrointestinal neoplasias. However, in these studies the role of ATOH1 in mediating these effects of Notch inhibitors was not examined. Here we test the hypothesis that GSI mediated Notch inhibition critically requires ATOH1, in normal and cancer cells, for growth arrest and differentiation into secretory cells.

## Materials and Methods

Complete materials and methods are available in the online supplementary methods.

### Mice and treatments

*Atoh1*<sup>WT</sup>, *Atoh1* <sup>$\Delta$ intestine</sup>, *APC*<sup>min</sup> and *APC*<sup>min</sup>; *Atoh1* <sup>$\Delta$ intestine</sup> mice were treated either with vehicle or Gamma secretase inhibitor-20 (GSI-20; EMD) at 10 $\mu$ M/kg once (1 $\times$ GSI) or twice (2 $\times$ GSI) a day for five days.

### Immunohistochemistry

Sections were stained for BrdU (Developmental Studies Hybridoma Bank), cleaved caspase-3 (Cell Signaling Technology), lysozyme (Invitrogen) and chromogranin A (ImmunoStar incorporated). Two-way ANOVA and Bonferroni posthoc analysis was used to measure significance (for BrdU and C-caspase-3 analysis).

### Cell culture and treatments

HCT116, HT29, LOVO, LS174T, RKO, and SW480 were treated with DMSO or 5 $\mu$ M DAPT (SIGMA) for four days. Non-targeting and ATOH1-shRNA constructs (SIGMA) packaged into lentivirus were used to infect cells before treatment. Cell Counting-8 Kit (Dojindo) and BrdU cell proliferation kit (Millipore) were used to measure proliferation.

### Immunoblotting

CRC cell and intestinal protein lysates were used for immunoblotting. The following antibodies were used mouse IgM anti-actin (Developmental Studies Hybridoma Bank), rabbit polyclonal anti-HES1 (Dr. Nadean Brown, Cincinnati Children's Hospital), rabbit polyclonal anti-cleaved Notch 1 (Val1744; Cell Signaling Technology), mouse monoclonal anti-Notch1 (mN1A; Santa Cruz Biotechnology), mouse monoclonal anti-p27[Kip1] (BD Transduction Laboratories) rabbit polyclonal anti-TFF3 (Dr. Daniel Podolsky, University of Texas), and rabbit polyclonal anti-poly-ADP ribose polymerase (PARP) (Cell Signaling Technology).

### Quantitative (q)RT-PCR

CRC cells treated with DMSO or DAPT (and shRNA) were harvested and used for RNA purification (Qiagen), DNase digestion, cDNA synthesis (Invitrogen) and SYBR Green-based qRT-PCR (Stratagene). A similar procedure was used for qRT-PCR from intestinal tissues treated with vehicle or GSI (GSI-20, 10 $\mu$ M/kg once a day for five days). The primers for the qRT-PCR are listed in the supplementary Tables 1 and 2. Two tailed Student's T-test and two-way ANOVA with Bonferroni posthoc test was used for bivariate analysis.

## Results

### Atoh1 is required for the effects of Notch inhibition on differentiation in the intestine

To genetically determine the role of Atoh1 in mediating the effects of Notch inhibition in the intestine, we treated *Wild type* (WT) and *Atoh1* <sup>$\Delta$ intestine</sup> mice with vehicle or GSI. GSI

treatment effectively inhibited Notch activation, as determined by a significant decrease in NICD (supplementary Figure 2). *Atoh1*<sup>*Δintestine*</sup> mice are mosaic, such that in the distal ileum and colon they harbor ~75% *Atoh1*-null crypts that lack all secretory cells, with ~25% of adjacent crypts retaining a functional copy of *Atoh1* (*Atoh1*-WT crypts)<sup>26</sup>. Histological analysis of intestines from *WT* and *Atoh1*<sup>*Δintestine*</sup> mice treated with vehicle or GSI showed no overt architectural changes to the mucosa in any of the mice (Figure 1A). Next, we stained the carbohydrate-rich goblet cell mucins with PAS/Alcian blue. As expected<sup>1, 17–19</sup>, GSI treatment of *WT* mice results in a dramatic increase in the number of goblet cells in the distal ileum (Figure 1B). However, neither vehicle-nor GSI-treated *Atoh1*-null crypts produced goblet cells, confirming the requirement of *Atoh1* for goblet cell differentiation and indicating that GSI treatment cannot overcome this requirement. Similarly, GSI treatment of *WT* animals results in increased production of Paneth cells (stained for Lysozyme; Figure 1C) and enteroendocrine cells (stained for Chromogranin A; Figure 1D). GSI treatment of *Atoh1*-null crypts shows no such increase in Paneth nor enteroendocrine cell differentiation (Figure 1C and D). Similar results for goblet and enteroendocrine cells were observed in the colon (data not shown). Of note, the remaining *Atoh1*-WT crypts in GSI-treated *Atoh1*<sup>*Δintestine*</sup> mice showed similar increases in secretory lineage cells as shown for *WT* mice, indicating a cell-autonomous role for *Atoh1* in mediating these effects (data not shown). Gene expression analyses of ileum and colon from GSI treated *WT* and *Atoh1*<sup>*Δintestine*</sup> mice confirmed these observations: *Atoh1* and secretory cell markers (*Agr2*, *Spink4*, *Tff3*) and differentiation factors (*Insm1*, *Spdef*) were upregulated by GSI treatment of *WT* mice, but were dramatically reduced in *Atoh1*<sup>*Δintestine*</sup> mice (Figure 2). We also observed reduced expression of the Notch target *Hes1* in the ileum of GSI treated *WT* mice, but no effect in GSI treated *Atoh1*<sup>*Δintestine*</sup> mice. Interestingly, we observed increased colonic expression of the Notch ligand *Dll1* in GSI-treated *WT* mice, which was also dependent upon *Atoh1* for its expression. Together, these results demonstrate that *Atoh1* is critically required for the effects of Notch/ $\gamma$ -secretase inhibitors on intestinal epithelial differentiation.

We next tested if Notch inhibition resulted in upregulation of *ATOHI* and markers of secretory cell differentiation in human CRC cells, in a manner similar to the effect in mouse adenomas<sup>1</sup>. We chose the mucinous adenocarcinoma cell line LS174T, which was reported to express low but detectable levels of *ATOHI* mRNA<sup>12</sup>, to characterize the effect of Notch inhibition and the role of *ATOHI* in regulating secretory cell marker expression. Figure 3A shows an increase in mucin production after GSI treatment compared to DMSO vehicle, evident by increased Alcian blue staining of the cells. A time course study of GSI treatment showed significant accumulation of *ATOHI* mRNA levels over 4 days (Figure 3B). Notch activation was inhibited as indicated by loss of the activated form of Notch (NICD; Figure 3D) and down regulation of its transcriptional target *HES1* (Figure 3B and 3D). Several secretory cell mRNAs were upregulated, including the goblet cell markers *SPDEF*, *MUC2*, *RETNLB* and *SPINK4*; and the enteroendocrine progenitor cell marker *NEUROG3* (Figure 3B). The secreted goblet cell protein TFF3 was similarly upregulated upon GSI treatment of LS174T cells (Figure 3D). The accumulation of secretory cell mRNAs correlated with the accumulation of *ATOHI* mRNA. Interestingly, *ATOHI* mRNA accumulation also correlated with increased expression of *DLL1* (Figure 3B). Thus Notch/ $\gamma$ -secretase inhibition in CRC cells activates expression of *ATOHI* and secretory cell markers.

Next, we tested whether upregulation of *ATOHI* upon Notch inhibition is required for activation of secretory cell markers. We measured the effect on GSI-induced gene expression of two different shRNAs that specifically reduce *ATOHI* expression. Figure 3C shows 30–40% reduction in GSI-induced *ATOHI* mRNA levels following shRNA treatment. Knockdown of endogenous *ATOHI* expression in these cells results in upregulation of *HES1* mRNA levels as shown for day 0 and day 4 for the vehicle treatment

(Figure 3C). *HES1* levels are reduced following GSI treatment in both non-targeting (control) and *ATOH1*-targeting shRNA treatments. The secretory cell markers *SPDEF*, *MUC2* and *NEUROG3* are significantly reduced with the *ATOH1* shRNA knockdown but not in the non-targeting shRNA treatments (Figure 3C). Similarly, *DLL1* levels are also reduced with *ATOH1* shRNA knockdown (Figure 3C). These data indicate 1) that *ATOH1* and *HES1* are reciprocally regulated, and 2) that *ATOH1* is required for secretory cell gene activation by Notch/ $\gamma$ -secretase inhibitors in LS174T colon cancer cells.

### **Atoh1 is required for the effects of Notch inhibition on intestinal proliferation and apoptosis**

Notch/ $\gamma$ -secretase inhibitors have been reported to reduce proliferation and enhance apoptosis of intestinal epithelial cells *in vivo*<sup>1, 17, 20</sup>. To test whether these effects of GSI are dependent upon *Atoh1*, *WT* and *Atoh1<sup>Aintestine</sup>* mice were treated with vehicle or GSI and the effect on proliferation and apoptosis was measured in both the distal ileum and colon. Consistent with previous reports, GSI treatment showed a 20–50% reduction in proliferating crypt cells both in *WT* mice and in *Atoh1-WT* crypts from *Atoh1<sup>Aintestine</sup>* animals, with no difference between these two control groups (Figure 4; white and grey bars, respectively). By contrast, *Atoh1-null* crypts treated with GSI did not show reduced proliferation and in fact we observed higher proliferation in 2×GSI treated *Atoh1-null* colon crypts (Figure 4; black bars). A similar pattern of GSI-induced, *Atoh1*-dependent reduction in proliferation was observed in both ileum and colon (Figure 4B and D). This striking difference in proliferative response to GSI was particularly apparent in *Atoh1<sup>Aintestine</sup>* mice where *Atoh1-WT* and *Atoh1-null* crypts appeared adjacent to each other (Figure 4A and C). We also noted higher levels of proliferation in the ileum of vehicle-treated *Atoh1-null* crypts compared to *WT* and *Atoh1-WT*, consistent with our previous reports<sup>13, 26</sup>. We next assessed GSI-induced apoptosis in ileum and colon sections by quantifying crypt cells stained by cleaved caspase 3 (CC3) in *WT* and *Atoh1<sup>Aintestine</sup>* mice. Ileal crypts showed a significant increase in CC3-positive cells in *WT* and *Atoh1-WT* crypts (Supplemental Figure 3A; white and grey bars), whereas *Atoh1-null* crypts showed no increase in apoptosis (Supplemental Figure 3A; black bars). A similar pattern of *Atoh1*-dependent, GSI-induced apoptosis was observed in the colon (Supplemental Figure 3B). Together, these results demonstrate that *Atoh1* mediates the effects of Notch/ $\gamma$ -secretase inhibitors on intestinal crypt progenitor proliferation and apoptosis.

### **ATOH1 induction is tightly correlated with the growth inhibitory effects of Notch inhibition in colorectal cancer cells**

Given the requirement for *Atoh1* to mediate the growth inhibitory properties of GSIs on normal intestinal cells (shown above), and recent reports that *ATOH1* functions as a tumor suppressor in colorectal cancers<sup>12–13</sup>, we next investigated the role of *ATOH1* in the growth inhibitory properties of GSIs in human CRC cell lines. We treated six different cell lines (LS174T, HT29, LOVO, RKO, SW480 and HCT116) for four days with vehicle or GSI to assess the effects on cell viability. Active Notch1 (NICD1) was significantly reduced upon GSI treatment in all cells where it was measurable (Figure 5A). LS174T cells showed the greatest reduction in cell viability when treated with GSI (~40%, Figure 5A). Similarly, HT29, LOVO, SW480 and HCT116 each showed small but significant reductions in viability when treated with GSI (10–20%, Figure 5A). In contrast, RKO showed no change in growth with GSI treatment compared to vehicle control (Figure 5A). We confirmed that these growth inhibitory effects of GSI were due to inhibition of proliferation with a BrdU incorporation assay: LS174T, LOVO, and HT29 cells showed a reduction in proliferation corresponding to reduced cell viability; RKO, SW480, and HCT116, which showed little or no effect of GSI on viability, showed no change in BrdU incorporation (Figure 5A). GSI can induce apoptosis *in vivo* (supplemental figure 3 A and B), therefore, we examined whether a



similar response is observed in CRC cells. Immunoblot analysis for cleavage of poly ADP-ribose polymerase (PARP), a marker of apoptosis, showed no increase in the major cleavage product upon GSI treatment, consistent with related reports<sup>21–22</sup> (Supplemental Figure 4). Thus, GSI treatment has variable potency to inhibit growth of CRC cell lines.

Next, we used GSI- and vehicle-treated CRC cells to quantify Notch pathway related mRNA levels. With few exceptions, *NOTCH* receptor and *JAGGED* ligand expression was unchanged by GSI treatment (Table 1). *HES1* expression was reduced by GSI treatment of LS174T, LOVO, and RKO cells, but did not correlate closely with NICD1 expression in all cell lines (Table 1 and Figure 5A). *ATOHI* induction by GSI was greatest in LS174T cells (~16 fold), whereas HT29 and LOVO cells showed modest induction, and RKO, SW480, and HCT116 had very low basal *ATOHI* expression and no induction upon GSI treatment (Table 1). Interestingly, only those cells that induced *ATOHI* upon GSI treatment increased expression of *MUC2*, *DLL1*, and *DLL4*. In contrast, *HES1* repression was not tightly correlated to this response (see HT29 and RKO cells). Thus, *ATOHI* expression was the best predictor of GSI-dependent gene expression changes.

Given the effect of GSI on proliferation and the concomitant upregulation of *ATOHI* mRNA levels, we wanted to examine the relationship between the GSI-induced growth inhibition and increased *ATOHI* expression. Using a log-linear comparison of the GSI effect on cell growth versus *ATOHI* expression for each CRC cell line, regression was used to derive a model (shown in Figure 5B) for which the coefficient of determination,  $R^2 = 0.93$ . These data suggest a strong inverse relationship between GSI-induced *ATOHI* expression and growth inhibition in CRC cells.

### **Atoh1 is required for the growth inhibitory effects of Notch inhibition on intestinal adenomas**

Previous studies showed that GSI treatment of small intestinal adenomas reduced proliferation and enhanced differentiation into goblet cells<sup>1</sup>. We examined whether these effects require *Atoh1* in GSI treated *APC<sup>min</sup>* and *APC<sup>min</sup>; Atoh1<sup>Δintestine</sup>* adenomas<sup>13</sup>. First, we assessed goblet cell differentiation by Alcian blue/PAS staining of GSI treated *APC<sup>min</sup>* and *APC<sup>min</sup>; Atoh1<sup>Δintestine</sup>* adenomas (for reference, H&E stained sections of these adenomas are shown in Supplemental Figure 5). Small intestinal adenomas from *APC<sup>min</sup>* mice treated with GSI showed enhanced goblet cell differentiation (Figure 6C). In contrast, goblet cells were absent in *Atoh1-null* ileal adenomas both in vehicle and GSI treated *APC<sup>min</sup>; Atoh1<sup>Δintestine</sup>* mice (Figure 6C). Similarly, colonic *APC<sup>min</sup>* adenomas showed an increase in goblet cell differentiation upon GSI treatment, but no such induction was observed in *Atoh1-null* colonic adenomas (Figure 6D). Given the *Atoh1*-dependent increased apoptosis in GSI treated ileal and colonic crypts (Supplemental Figure 3A and B), we examined the effect of GSI treatment on *APC<sup>min</sup>* and *APC<sup>min</sup>; Atoh1<sup>Δintestine</sup>* adenomas. In agreement with our previous finding that *ATOHI* regulates apoptosis in cancer cells<sup>13</sup>, we find that *Atoh1-null* adenomas contain less apoptotic cells than control tumors (supplemental Figure 3C and D). However, in contrast to normal crypts we found no induction of apoptosis upon treatment with GSI in ileal or colonic adenomas, regardless of *Atoh1* genotype (supplemental Figure 3C and D).

Finally, we measured proliferation by BrdU incorporation of neoplastic cells in adenomas from the colon and small intestine (Supplemental Figure 6). We observed higher proliferation in *Atoh1-null* ileal adenomas compared to *Atoh1-WT* adenomas (Figure 6A). Quantitation of BrdU-positive cells showed a significant 20–25% reduction in proliferation in GSI-treated adenomas from the small intestine of *APC<sup>min</sup>* mice and from *Atoh1-WT* adenomas in the proximal small intestine of *APC<sup>min</sup>; Atoh1<sup>Δintestine</sup>* mice (Figure 6A). Similar analysis showed a complete absence of effect of GSI on proliferation in *Atoh1-null*

ileal adenomas from *APC<sup>min</sup>; Atoh1<sup>Δintestine</sup>* mice (Figure 6A). In the colon, there was a pronounced 45% reduction in proliferation in GSI treated *APC<sup>min</sup>* adenomas compared to vehicle treated colon adenomas (Figure 6B). In contrast, *Atoh1-null* colonic adenomas from *APC<sup>min</sup>; Atoh1<sup>Δintestine</sup>* mice treated with GSI showed no such reduction in proliferation (Figure 6B). Thus *Atoh1* is essential for differentiation and growth inhibition by Notch/ $\gamma$ -secretase inhibitors in intestinal tumors.

## Discussion

In this study we show that ATOH1 is critically required for all effects of Notch/ $\gamma$ -secretase inhibitors on intestinal progenitor cells. Our results suggest a model in which the primary function of Notch in intestinal stem cells is to prevent ATOH1 expression: when Notch is inhibited, ATOH1 is activated and drives cell cycle arrest, apoptosis, and terminal differentiation of progenitors into secretory cells. When both Notch and ATOH1 are inhibited, no change in proliferation or apoptosis is observed, and absorptive enterocyte differentiation proceeds normally. Therefore, Notch has no unique function in intestinal progenitors other than to regulate appropriate ATOH1 expression.

Our findings provide new insights into the mechanism of Notch signaling in the intestine. We found that *Delta-like* Notch ligands are targets of ATOH1 activation in the intestine (Figures 2 & 3, Table 1). These ligands likely mediate lateral inhibition in the crypts (e.g., restriction of a subset of progenitors to the secretory fate), as shown in the zebrafish intestine<sup>27</sup>. Interestingly, we found that *Jagged* ligands were not regulated by Notch-ATOH1 (Table 1 and unpublished observations), consistent with previous reports that they are targets of the WNT/ $\beta$ -catenin pathway<sup>28</sup>. Whether differential responses to distinct Notch ligands regulates the fate of differentiating progenitors or “quiescent” label-retaining stem cells versus “active” crypt-base columnar stem cells is an outstanding question for future investigation. We also found that reduction of ATOH1 induced *HES1* expression in a Notch-dependent manner (Figure 3C). This indicates that ATOH1 and Notch reciprocally inhibit one another, suggesting a model of cell fate determination by lateral inhibition in which reciprocal inhibition and positive autoregulation combine to lock in secretory versus absorptive progenitor status.

Our results confirm that ATOH1 is critical for normal differentiation and homeostasis of intestinal progenitors<sup>4, 26</sup>. Recently, the cell cycle inhibitor p27<sup>Kip1</sup> was identified as a target of Notch repression via Hes1, and was found to be de-repressed upon GSI treatment<sup>9</sup>. We found reduced p27 expression in *Atoh1*-mutant colons, which was not restored by Notch inhibition (Supplementary Figure 2 and Bossuyt et al<sup>13</sup>). Together, these data suggest a model for regulation of intestinal progenitor proliferation where p27 expression is activated by *Atoh1* and repressed by Hes1. De-repression of p27 as a result of Notch/Hes1 inhibition allows increasing *Atoh1* to enhance p27 expression and block proliferation. In *Atoh1*-null cells, reduced p27 is associated with increased proliferation; de-repression of p27 by Notch/Hes1 inhibition is insufficient without coordinate activation of p27 by *Atoh1*, and thus proliferation is maintained.

Our findings support the hypothesis that ATOH1's tumor suppressive function<sup>12-13, 29</sup> is mediated by its effects on intestinal progenitors and/or cancer stem cells. Consistent with this tumor suppressive function, we find hyperproliferation and reduced apoptosis of *Atoh1-null* adenomas (Figure 6 and supplemental Figure 3). Of note, cancer cells respond to GSI not by inducing apoptosis but instead by reducing proliferation in an *Atoh1*-dependent manner (compare normal progenitors in Figure 4 and Supplemental Figure 3 to cancer cells in Figures 5 and 6 and Supplemental Figure 3 and 4). *Atoh1*-dependent, GSI-induced cell cycle arrest may enhance tumor cell killing by cytotoxic drugs<sup>21-23</sup>; whether ATOH1

mediates the synergistic effect of GSI and chemotherapeutics should be examined in the future.

Our results have several therapeutic implications. GSI therapy for non-intestinal malignancies and other diseases has been limited due to toxicity in the intestine<sup>18, 30</sup>. Our results suggest that targeted reduction of ATOH1 may prevent these side effects, and also that the expression level of ATOH1 is predictive of any approach to mitigating intestinal toxicity. As one approach to mitigate intestinal toxicity of GSIs, Real *et al.* showed that glucocorticoid treatment blocked the effects of GSIs in the intestine while enhancing the anti-leukemic and lymphoid effects<sup>30</sup>. The ability of glucocorticoid to block intestinal toxicity of GSIs was suggested to be mediated by downregulation of the transcription factor Klf4; whether Atoh1 is involved in this process remains to be determined. Recently, Notch-sparing GSIs have been developed to selectively inhibit processing of A $\beta$  in Alzheimer's disease<sup>16</sup>. We suggest that ATOH1 expression may be a useful functional marker of intestinal side effects when determining the relative selectivity of the GSIs for A $\beta$  over Notch. Among GI malignancies, we show that ATOH1 is a critical mediator of GSI effects. Therefore, the ability to induce ATOH1 is key for these therapies to be effective. Importantly, we recently showed that ATOH1 is silenced in ~80% of sporadic colorectal cancers<sup>13</sup>; therefore GSI therapy of these silenced tumors will be ineffective since they lack expression of the critical mediator of GSI treatment (*ATOH1*). To utilize GSIs in GI malignancies, we suggest that patients should first be stratified according to ATOH1 silencing status. For example, we predict that ~20% of CRCs that retain ATOH1 expression will respond to GSI therapy. Furthermore, we predict that gastric and esophageal tumors will respond to GSI therapy when they include ATOH1-positive intestinal metaplasia, but will become resistant to GSI therapy if they progress further and silence ATOH1. Together, our results demonstrate that ATOH1 is essential for all effects of Notch/ $\gamma$ -secretase inhibitors in normal and cancerous intestinal cells, and suggest that selective targeting of ATOH1 will allow for tissue specific therapeutic modalities. More broadly, our results support the concept of targeting tissue-specific differentiation factors as an important approach to inhibiting growth of cancers.

## Supplementary Material

Refer to Web version on PubMed Central for supplementary material.

## Acknowledgments

This study was supported by NIH grants T35 DK060444, K01 DK071686, R01 CA142826, and P30 DK078392; an American Cancer Society-Ohio Chapter pilot award; and an American Gastroenterology Association/FDHN Research Scholars Award.

We thank Jefferson Vallance, Tasneem Kaleem, and Allison Price for their technical assistance; Dr. Nadean Brown (Cincinnati Children's Hospital) for providing the Hes1 polyclonal antibody; Dr. Daniel Podolsky (University of Texas Southwestern Medical School) for anti-TFF3 rabbit polyclonal antibody. This work was supported by a pilot award from the Cincinnati Digestive Health Center supported by P30 DK078392, a Foundation for Digestive Health and Nutrition Research Scholars Award, National Institutes of Health (NIH) K01 DK071686, R01 CA142826, and American Cancer Society (Ohio Affiliate) Pilot Award to NFS. DB was supported by a NIH institutional training award T35 DK060444.

## Abbreviations

|              |                   |
|--------------|-------------------|
| <b>ATOH1</b> | Atonal homolog 1  |
| <b>CRC</b>   | colorectal cancer |
| <b>BrdU</b>  | Bromodeoxyuridine |



|               |   |
|---------------|---|
| <b>RT-PCR</b> | reverse-transcriptase-PCR   |
| <b>CC3</b>    | Cleaved caspase 3   |
| <b>APC</b>    | adenomatosis polyposis coli   |
| <b>min</b>    | multiple intestinal neoplasia   |
| <b>HES1</b>   | Hairy/Enhancer of Split 1   |
| <b>GSI</b>    | $\gamma$ -secretase inhibitor   |
| <b>DAPT</b>   | N-[N-(3,5-difluorophenacetyl)-l-alanyl]-S-phenylglycine t-butyl ester |
| <b>PAS</b>    | periodic acid Schiff's  |
| <b>NICD</b>   | Notch IntraCellular Domain  |
| <b>SPDEF</b>  | SAM Pointed Domain containing ETS transcription Factor                |
| <b>MUC2</b>   | MUCIN2  |
| <b>RETNLB</b> | Resistin Like B   |
| <b>SPINK4</b> | Serine Peptidase Inhibitor, Kazal type 4                              |
| <b>TFF3</b>   | TreFoil Factor 3  |
| <b>DLL1</b>   | Delta Like 1  |
| <b>DLL4</b>   | Delta Like 4  |
| <b>JAG1</b>   | Jagged 1  |
| <b>JAG2</b>   | Jagged 2  |
| <b>cPARP</b>  | cleaved poly-ADP ribose polymerase                                    |
| <b>Agr2</b>   | Anterior gradient homolog2  |
| <b>Insm1</b>  | Insulinoma-associated 1   |

## References

1. van Es JH, van Gijn ME, Riccio O, van den Born M, Vooijs M, Begthel H, Cozijnsen M, Robine S, Winton DJ, Radtke F, Clevers H. Notch/ $\gamma$ -secretase inhibition turns proliferative cells in intestinal crypts and adenomas into goblet cells. *Nature*. 2005; 435:959–63. [PubMed: 15959515]
2. Feder JN, Li L, Jan LY, Jan YN. Genomic cloning and chromosomal localization of HRY, the human homolog to the *Drosophila* segmentation gene, hairy. *Genomics*. 1994; 20:56–61. [PubMed: 8020957]
3. Ben-Arie N, McCall AE, Berkman S, Eichele G, Bellen HJ, Zoghbi HY. Evolutionary conservation of sequence and expression of the bHLH protein Atonal suggests a conserved role in neurogenesis. *Hum Mol Genet*. 1996; 5:1207–16. [PubMed: 8872459]
4. Yang Q, Bermingham NA, Finegold MJ, Zoghbi HY. Requirement of Math1 for secretory cell lineage commitment in the mouse intestine. *Science*. 2001; 294:2155–8. [PubMed: 11739954]
5. Jensen J, Pedersen EE, Galante P, Hald J, Heller RS, Ishibashi M, Kageyama R, Guillemot F, Serup P, Madsen OD. Control of endodermal endocrine development by Hes-1. *Nat Genet*. 2000; 24:36–44. [PubMed: 10615124]
6. Fre S, Huyghe M, Mourikis P, Robine S, Louvard D, Artavanis-Tsakonas S. Notch signals control the fate of immature progenitor cells in the intestine. *Nature*. 2005; 435:964–8. [PubMed: 15959516]
7. Stanger BZ, Datar R, Murtaugh LC, Melton DA. Direct regulation of intestinal fate by Notch. *Proc Natl Acad Sci U S A*. 2005; 102:12443–8. [PubMed: 16107537]

8. Vooijs M, Ong CT, Hadland B, Huppert S, Liu Z, Korving J, van den Born M, Stappenbeck T, Wu Y, Clevers H, Kopan R. Mapping the consequence of Notch1 proteolysis in vivo with NIP-CRE. *Development*. 2007; 134:535–44. [PubMed: 17215306]
9. Riccio O, van Gijn ME, Bezdek AC, Pellegrinet L, van Es JH, Zimmer-Strobl U, Strobl LJ, Honjo T, Clevers H, Radtke F. Loss of intestinal crypt progenitor cells owing to inactivation of both Notch1 and Notch2 is accompanied by derepression of CDK inhibitors p27Kip1 and p57Kip2. *EMBO Rep*. 2008; 9:377–83. [PubMed: 18274550]
10. Bjerknes M, Cheng H. Gastrointestinal stem cells. II. Intestinal stem cells. *Am J Physiol Gastrointest Liver Physiol*. 2005; 289:G381–7. [PubMed: 16093419]
11. Baker NE, Yu S, Han D. Evolution of proneural atonal expression during distinct regulatory phases in the developing *Drosophila* eye. *Curr Biol*. 1996; 6:1290–301. [PubMed: 8939576]
12. Leow CC, Romero MS, Ross S, Polakis P, Gao WQ. Hath1, down-regulated in colon adenocarcinomas, inhibits proliferation and tumorigenesis of colon cancer cells. *Cancer Res*. 2004; 64:6050–7. [PubMed: 15342386]
13. Bossuyt W, Kazanjian A, De Geest N, Van Kelst S, De Hertogh G, Geboes K, Boivin GP, Luciani J, Fuks F, Chuah M, VandenDriessche T, Marynen P, Cools J, Shroyer NF, Hassan BA. Atonal homolog 1 is a tumor suppressor gene. *PLoS Biol*. 2009; 7:e39. [PubMed: 19243219]
14. Wolfe MS, Citron M, Diehl TS, Xia W, Donkor IO, Selkoe DJ. A substrate-based difluoro ketone selectively inhibits Alzheimer's gamma-secretase activity. *J Med Chem*. 1998; 41:6–9. [PubMed: 9438016]
15. De Strooper B, Annaert W, Cupers P, Saftig P, Craessaerts K, Mumm JS, Schroeter EH, Schrijvers V, Wolfe MS, Ray WJ, Goate A, Kopan R. A presenilin-1-dependent gamma-secretase-like protease mediates release of Notch intracellular domain. *Nature*. 1999; 398:518–22. [PubMed: 10206645]
16. Augelli-Szafran CE, Wei HX, Lu D, Zhang J, Gu Y, Yang T, Wolfe MS. Discovery of Notch-Sparing gamma-Secretase Inhibitors. *Curr Alzheimer Res*. 2010
17. Milano J, McKay J, Dagenais C, Foster-Brown L, Pognan F, Gadiant R, Jacobs RT, Zacco A, Greenberg B, Ciaccio PJ. Modulation of notch processing by gamma-secretase inhibitors causes intestinal goblet cell metaplasia and induction of genes known to specify gut secretory lineage differentiation. *Toxicol Sci*. 2004; 82:341–58. [PubMed: 15319485]
18. Searfoss GH, Jordan WH, Calligaro DO, Galbreath EJ, Schirtzinger LM, Berridge BR, Gao H, Higgins MA, May PC, Ryan TP. Adipsin, a biomarker of gastrointestinal toxicity mediated by a functional gamma-secretase inhibitor. *J Biol Chem*. 2003; 278:46107–16. [PubMed: 12949072]
19. Wong GT, Manfra D, Poulet FM, Zhang Q, Josien H, Bara T, Engstrom L, Pinzon-Ortiz M, Fine JS, Lee HJ, Zhang L, Higgins GA, Parker EM. Chronic treatment with the gamma-secretase inhibitor LY-411,575 inhibits beta-amyloid peptide production and alters lymphopoiesis and intestinal cell differentiation. *J Biol Chem*. 2004; 279:12876–82. [PubMed: 14709552]
20. Ghaleb AM, Aggarwal G, Bialkowska AB, Nandan MO, Yang VW. Notch inhibits expression of the Kruppel-like factor 4 tumor suppressor in the intestinal epithelium. *Mol Cancer Res*. 2008; 6:1920–7. [PubMed: 19074836]
21. Akiyoshi T, Nakamura M, Yanai K, Nagai S, Wada J, Koga K, Nakashima H, Sato N, Tanaka M, Katano M. Gamma-secretase inhibitors enhance taxane-induced mitotic arrest and apoptosis in colon cancer cells. *Gastroenterology*. 2008; 134:131–44. [PubMed: 18166351]
22. Aleksic T, Feller SM. Gamma-secretase inhibition combined with platinum compounds enhances cell death in a large subset of colorectal cancer cells. *Cell Commun Signal*. 2008; 6:8. [PubMed: 18950493]
23. Meng, RD.; Shelton, CC.; Li, Y.; Schwartz, GK. Effect of targeting the Notch developmental pathway in metastatic gastric cancers on growth suppression, apoptosis, and chemosensitivity. 2009 American Society for Clinical Oncology Gastrointestinal Cancers Symposium; 2009. p. Abstract 25
24. Konturek P, Burnat G, Rau T, Hahn EG. Implication of Notch signaling and CDX-2 Expression in Barrett's Canrinogenesis. *Digestive Diseases Week*. 2008:Abstract 996.
25. Aster JC. Deregulated NOTCH signaling in acute T-cell lymphoblastic leukemia/lymphoma: new insights, questions, and opportunities. *Int J Hematol*. 2005; 82:295–301. [PubMed: 16298817]

26. Shroyer NF, Helmrath MA, Wang VY, Antalffy B, Henning SJ, Zoghbi HY. Intestine-Specific Ablation of Mouse atonal homolog 1 (Math1) Reveals a Role in Cellular Homeostasis. *Gastroenterology*. 2007; 132:2478–88. [PubMed: 17570220]
27. Crosnier C, Vargesson N, Gschmeissner S, Ariza-McNaughton L, Morrison A, Lewis J. Delta-Notch signalling controls commitment to a secretory fate in the zebrafish intestine. *Development*. 2005; 132:1093–104. [PubMed: 15689380]
28. Rodilla V, Villanueva A, Obrador-Hevia A, Robert-Moreno A, Fernandez-Majada V, Grilli A, Lopez-Bigas N, Bellora N, Alba MM, Torres F, Dunach M, Sanjuan X, Gonzalez S, Gridley T, Capella G, Bigas A, Espinosa L. Jagged1 is the pathological link between Wnt and Notch pathways in colorectal cancer. *Proc Natl Acad Sci U S A*. 2009; 106:6315–20. [PubMed: 19325125]
29. Tsuchiya K, Nakamura T, Okamoto R, Kanai T, Watanabe M. Reciprocal targeting of Hath1 and beta-catenin by Wnt glycogen synthase kinase 3beta in human colon cancer. *Gastroenterology*. 2007; 132:208–20. [PubMed: 17241872]
30. Real PJ, Tosello V, Palomero T, Castillo M, Hernando E, de Stanchina E, Sulis ML, Barnes K, Sawai C, Homminga I, Meijerink J, Aifantis I, Basso G, Cordon-Cardo C, Ai W, Ferrando A. Gamma-secretase inhibitors reverse glucocorticoid resistance in T cell acute lymphoblastic leukemia. *Nat Med*. 2009; 15:50–8. [PubMed: 19098907]

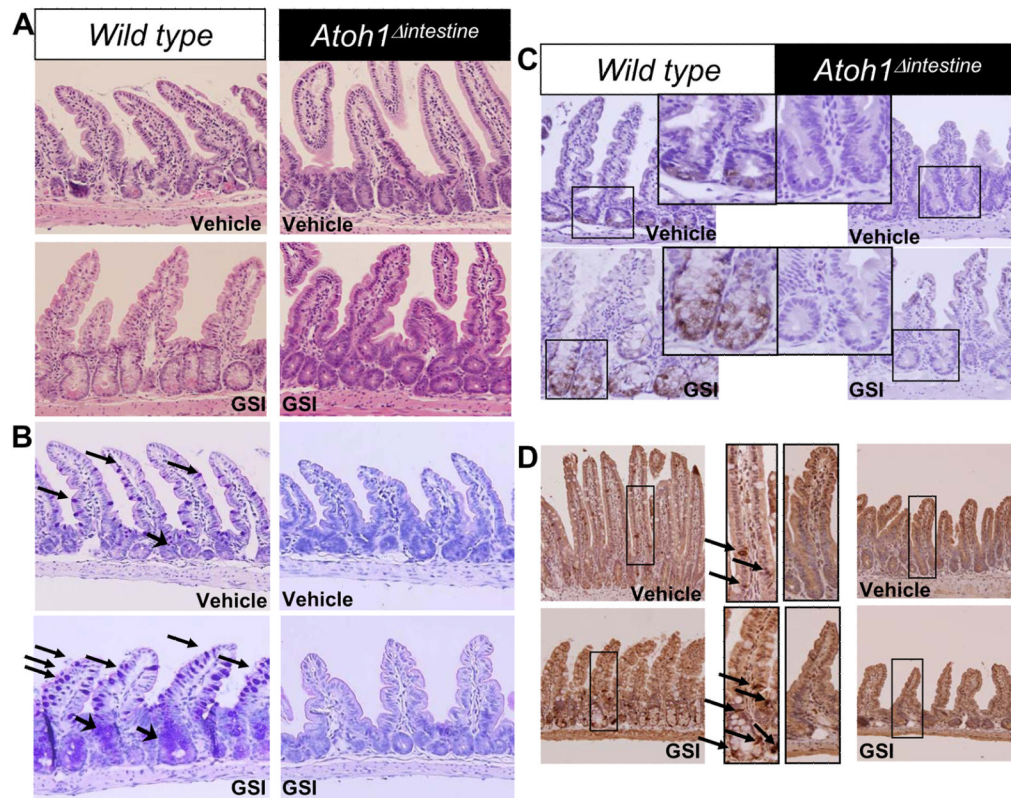


**Figure 1. *Atoh1* mediates GSI differentiation into secretory cells**

**A)** H&E staining of distal ileum. Vehicle and GSI treated (GSI-20, 10 μM/kg twice a day for 5 days) *Wild type* and *Atoh1*<sup>Δintestine</sup> mice. **B)** Alcian blue/PAS staining of ileal sections. Arrows point to goblet cells in the villi and crypts. **C)** lysozyme staining of paneth cells. Middle panels represent magnification of ileal crypts of the smaller highlighted boxes. **D)** Chromogranin staining of the ileal tissues. Middle panels represent magnification of the smaller highlighted boxes; arrow point to chromogranin positive cells.

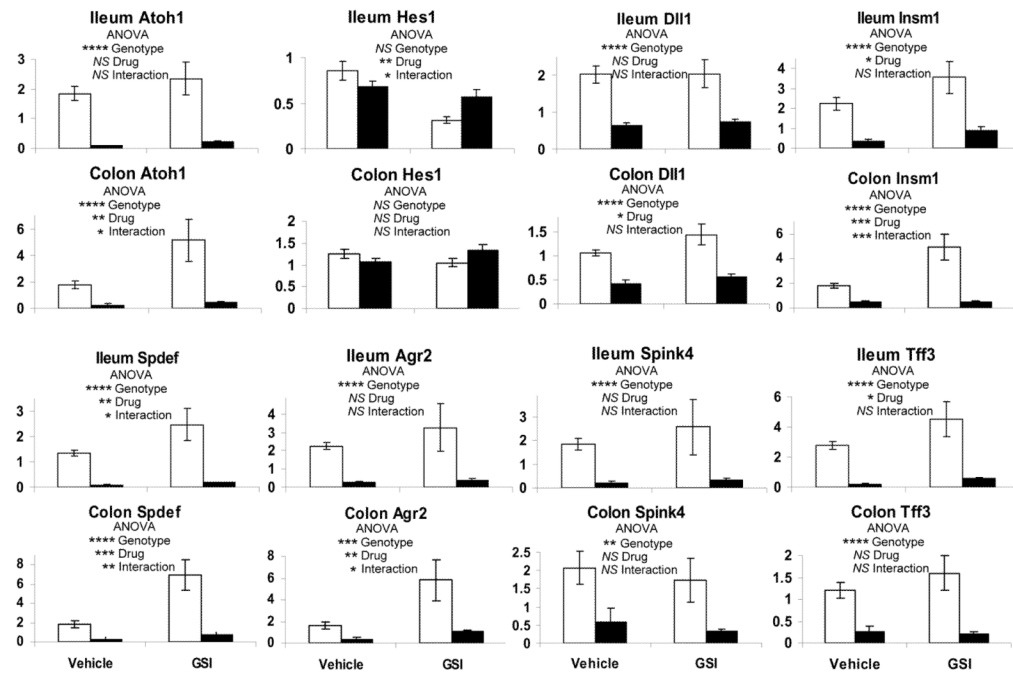


**Figure 2. Atoh1 mediates GSI-induced secretory cell gene expression in the intestine**  
 Quantitative RT-PCR for gene expression in ileal and colonic tissues treated with vehicle or GSI (10 $\mu$ M/kg once a day for five days), normalized to *Gapdh* expression. White bars represent WT tissues and black bars *Atoh1* <sup>$\Delta$ intestine</sup> tissues. P values shown were calculated using 2-way ANOVA for Drug (GSI) and Genotype (WT vs *Atoh1* <sup>$\Delta$ intestine</sup>) effects. \*  $p < 0.05$ , \*\*  $p < 0.001$ , \*\*\*  $p < 0.0001$ , \*\*\*\*  $p < 0.00001$ , NS (not significant). The error bars represent standard error of the mean.



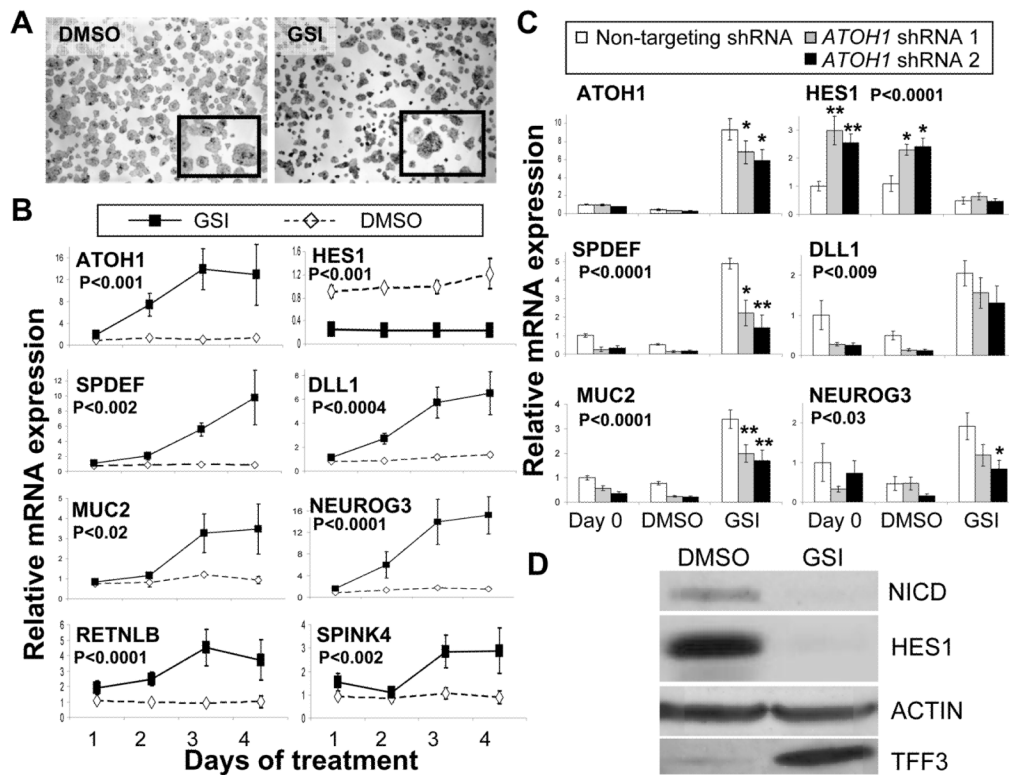


**Figure 3. ATOH1 mediates GSI-induced secretory cell gene expression in colon cancer cells**

**A)** Alcian blue/PAS staining of LS174T cells treated either with DMSO or GSI (5 $\mu$ M DAPT) for 4 days. The insets are higher magnification of stained cells. **B)** Quantitative RT-PCR for gene expression in LS174T cells treated with DMSO or GSI (5 $\mu$ M DAPT), normalized to expression at day 0. P values represent GSI effect using 2 way ANOVA analysis. **C)** Quantitative RT-PCR for gene expression in LS174T cells transduced with lentivirus encoding either non-targeting (white bars), or ATOH1-targeting (grey and black bars) shRNA, normalized to expression of cells transduced with non-targeting shRNA at day 0. 48 hours post transduction (Day 0) cells were treated with DMSO or GSI (5 $\mu$ M DAPT) for four days. P values shown were calculated using 2-way ANOVA for shRNA effect, Bonferroni posttests calculated individual group differences, \*  $p < 0.05$ , \*\*  $p < 0.001$ . The error bars represent standard error of the mean. **D)** A representative immunoblot of LS174T after 4 days of treatment with DMSO or GSI (5 $\mu$ M DAPT). Antibodies recognized the Notch intracellular domain (NICD), HES1, TFF3, and ACTIN (as a loading control).

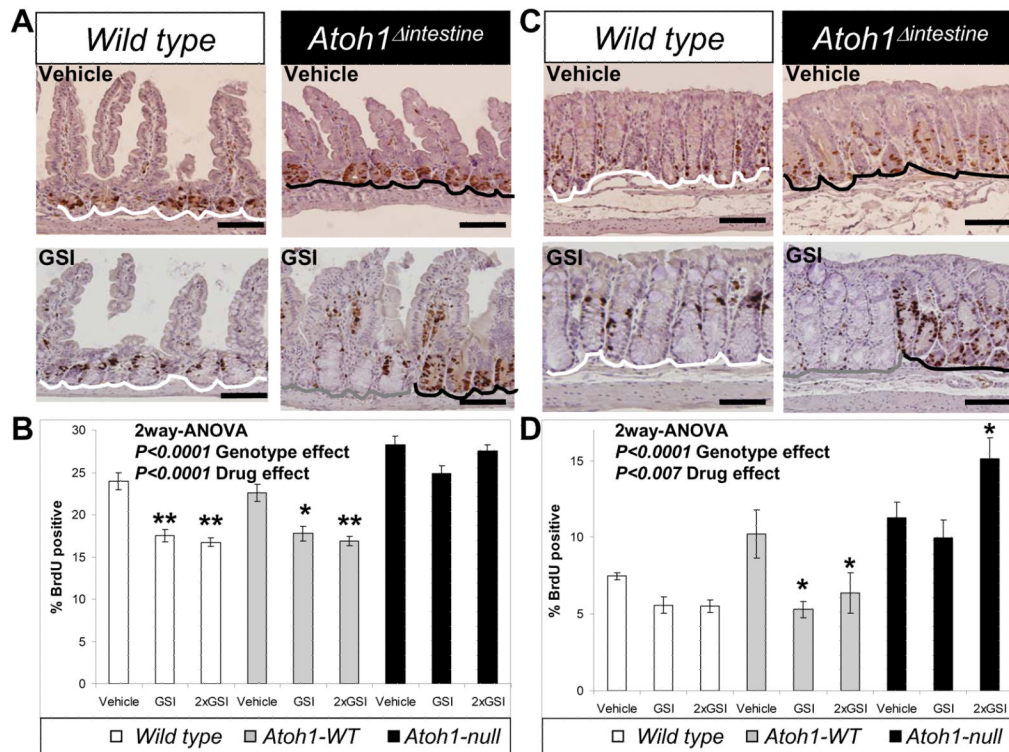


**Figure 4. Atoh1 mediates GSI-induced growth inhibition in normal intestinal epithelia**  
**A)** S-phase cells (marked by BrdU) were stained brown in ileal sections from *Wild type* and *Atoh1<sup>Δintestine</sup>* mice treated with vehicle or GSI (GSI-20, 10 $\mu$ M/kg twice a day for 5 days). White lines underline *Wild type* crypts from *Wild type* animals; grey line underlines *Atoh1-WT* crypts in *Atoh1<sup>Δintestine</sup>* mice and black lines underline *Atoh1-null* crypts in *Atoh1<sup>Δintestine</sup>* mice. **B)** Quantification of BrdU positive ileal cells from vehicle or GSI treated *Wild type* and *Atoh1<sup>Δintestine</sup>* mice. Animals were treated for 5 days with 10 $\mu$ M/kg once a day (GSI) or twice a day (2 $\times$ GSI). The white, grey and black bars represent counts from different set of crypts as described in **A**. [*Wild type* animals: n=5 for vehicle, n=4 for GSI, and n=7 for 2 $\times$ GSI; *Atoh1<sup>Δintestine</sup>* animals: n=4 for vehicle, n=8 for GSI, and n=5 for 2 $\times$ GSI]. A significant difference in proliferation was measured for vehicle treated *Wild type* versus *Atoh1-null* crypts ( $p < 0.01$ ), and *Atoh1-WT* versus *Atoh1-null* crypts ( $p < 0.001$ ). **C)** Colonic sections from mice as shown in **A**. **D)** Quantification of BrdU positive colonic cells from mice as shown in **B**. [*Wild type* animals: n=3 for vehicle, n=8 for GSI, and n=6 for 2 $\times$ GSI; *Atoh1<sup>Δintestine</sup>* animals: n=4 for vehicle, n=4 for GSI, and n=5 for 2 $\times$ GSI]. **(B and D)** Error bars represent standard error of the mean. Significance was calculated using 2-way ANOVA for GSI and genotype effects. Bonferroni posttest analysis was used for calculating significance for individual groups. \*  $p < 0.05$ , \*\*  $p < 0.001$ .

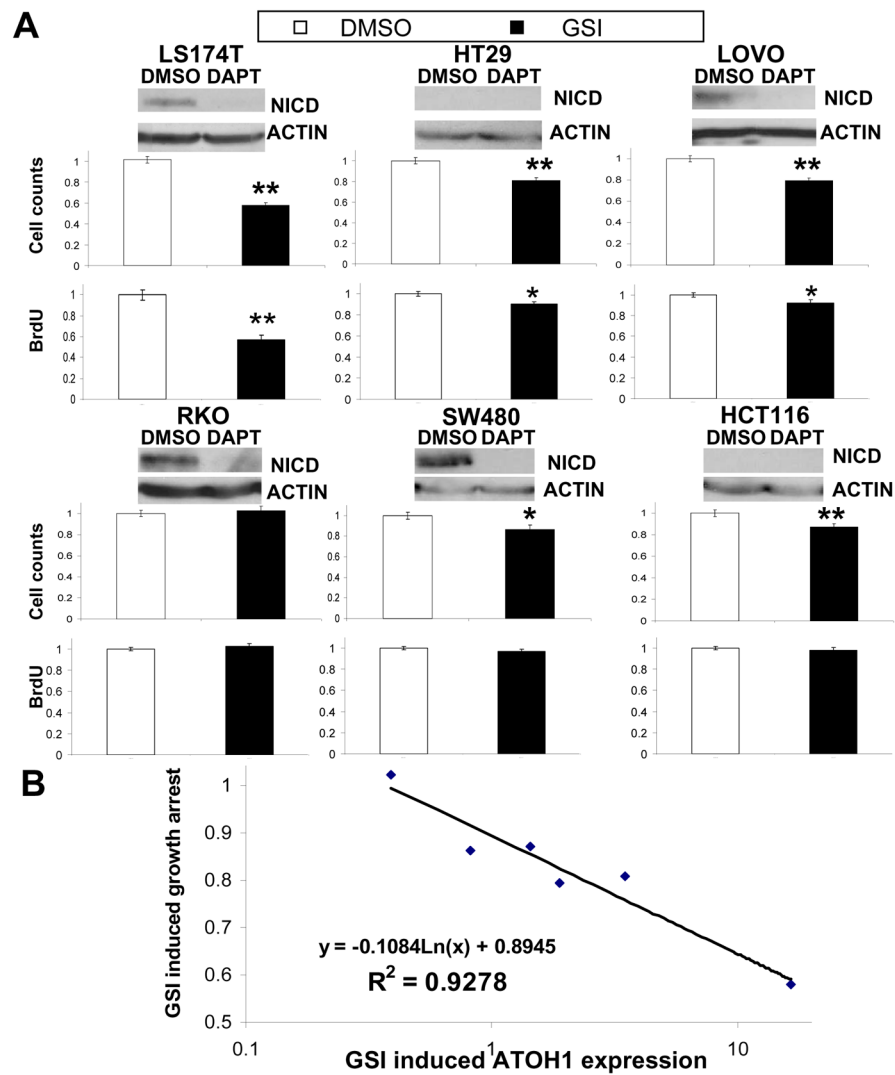


**Figure 5. GSI induced Atoh1 expression levels is associated with CRC growth inhibition**  
**A)** CRC cell lines are named above immunoblots and pairs of bar graphs representing cell growth (upper bar graph) and BrdU incorporation (lower bar graph) following 4 days of treatment with DMSO or GSI (5µM DAPT). Antibodies recognized the Notch intracellular domain (NICD), and ACTIN (as a loading control) for the representative immunoblots. Cell growth and proliferation were quantified by cell viability and BrdU incorporation assays and normalized to growth or BrdU incorporation of DMSO treated cells. **B)** log-linear comparison of the GSI effect on cell growth versus *ATOH1* expression (determined by quantitative RT-PCR, Table 1) for CRC cell lines. Linear regression was used to determine the model shown and to determine  $R^2$ . GSI induced ATOH1 expression represent the ratio of DMSO/DAPT for normalized expression levels of ATOH1. The GSI induced growth arrest represents the ratio of DMSO/DAPT for the normalized average cell count for each treatment. Error bars represent standard error of the mean. Significance was calculated using 2 tailed student T-tests comparing DMSO to GSI treatment. \*  $p < 0.05$ , \*\*  $p < 0.001$ .

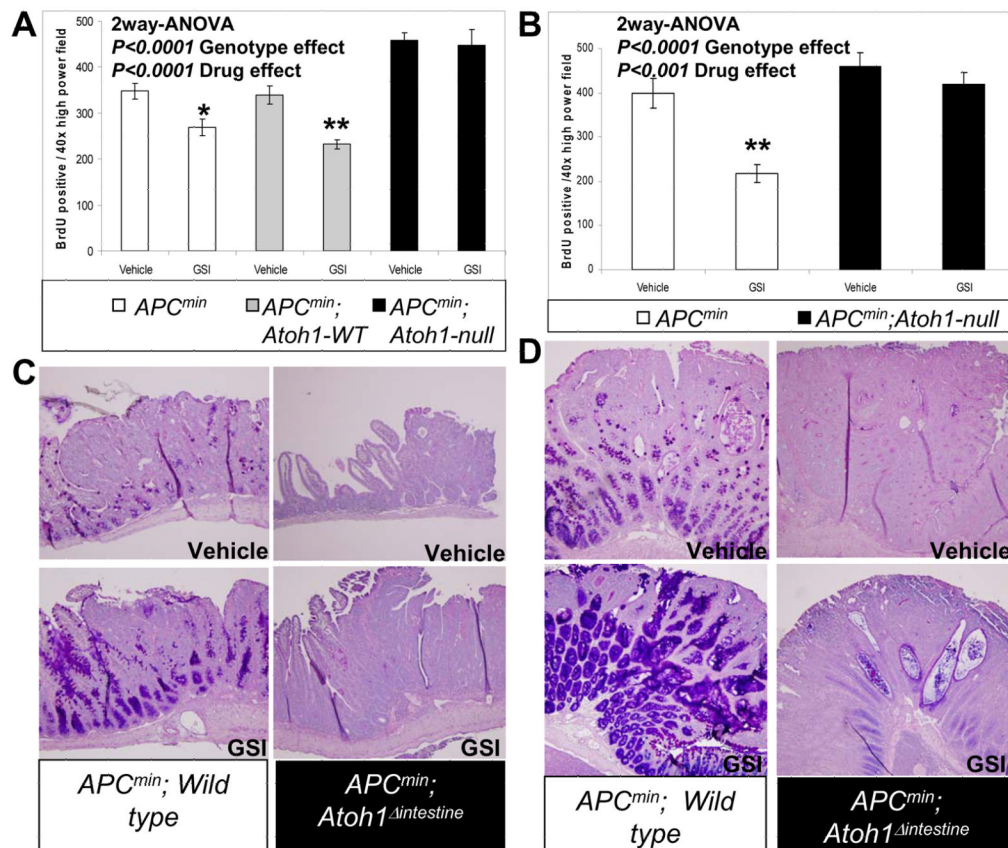


**Figure 6. Atoh1 mediates GSI-induced differentiation and growth inhibition in intestinal tumors**  
**A)** Quantification of proliferation in ileal adenomas from mice treated with vehicle or GSI (GSI-20, 10 $\mu$ M/kg twice a day for 5 days). White bars represent adenomas from  $APC^{min}$  animals. Grey bars represent  $Atoh1-WT$  adenomas in  $APC^{min}; Atoh1^{\Delta intestine}$  mice. Black bars represent  $Atoh1-null$  adenomas from  $APC^{min}; Atoh1^{\Delta intestine}$  mice. [ $APC^{min}$  adenomas: n=21 for vehicle, n=33 for GSI;  $APC^{min}; Atoh1-WT$  adenomas: n=27 for vehicle, n=25 for GSI;  $APC^{min}; Atoh1-null$  adenomas: n=15 for vehicle and n=14 for GSI] A significant difference in proliferation was measured for vehicle treated *Wild type* versus *Atoh1-null* adenomas ( $p < 0.001$ ), and *Atoh1-WT* versus *Atoh1-null* adenomas ( $p < 0.001$ ). **B)** Quantification of proliferation in colonic adenomas from mice treated with vehicle or GSI (GSI-20, 10 $\mu$ M/kg twice a day for 5 days). The color scheme for bars is the same as in **A**. [ $APC^{min}$  adenomas: n=9 for vehicle, n=16 for GSI;  $APC^{min}; Atoh1-null$  adenomas: n=10 for vehicle and n=19 for GSI]. Error bars represent standard error of the mean. Significance was calculated using 2-way ANOVA for GSI and genotype effects. Bonferroni posttest analysis was used for calculating significance for individual groups. \*  $p < 0.05$ , \*\*  $p < 0.001$ . **(C and D)** Representative Alcian blue/PAS staining of  $APC^{min}$  and  $APC^{min}; Atoh1-null$  ileal and colonic adenomas treated with vehicle and GSI (GSI-20, 10 $\mu$ M/kg twice a day for 5 days).

**Table 1**  
**Gene expression in Notch/ $\gamma$ -secretase inhibitor treated colorectal cancer cell lines**

2-tailed student T-Test was used to measure differences in gene expression between vehicle (DMSO) and  $\gamma$ -secretase inhibitor (DAPT) treatment (bold number pairs are significantly different,  $p < 0.05$ )

|        |      | ATOH1              | HES1             | MUC2                  | DLL1           | DLL4         | NOTCH1       | NOTCH2       | JAG1         | JAG2          |
|--------|------|--------------------|------------------|-----------------------|----------------|--------------|--------------|--------------|--------------|---------------|
| LS174T | DMSO | 1.1 +/- 0.1        | 1.6 +/- 0.1      | 2.0 +/- 0.05          | 1.2 +/- 0.02   | 0.8 +/- 0.2  | 0.6 +/- 0.1  | 0.4 +/- 0.07 | 5.5 +/- 0.9  | 0.09 +/- 0.03 |
|        | DAPT | 17.4 +/- 5.0       | 0.8 +/- 0.05     | 34.4 +/- 5.6          | 11.4 +/- 1.7   | 12.2 +/- 3.0 | 0.9 +/- 0.3  | 0.4 +/- 0.01 | 6.1 +/- 1.2  | 0.2 +/- 0.03  |
| HT29   | DMSO | 0.4 +/- 0.03       | 1.6 +/- 0.1      | 0.02 +/- 0.002        | 0.07 +/- 0.01  | 0.5 +/- 0.04 | 1.0 +/- 0.2  | 1.0 +/- 0.1  | 1.1 +/- 0.06 | 0.5 +/- 0.1   |
|        | DAPT | 1.4 +/- 0.1        | 1.5 +/- 0.08     | 0.1 +/- 0.02          | 0.4 +/- 0.06   | 1.7 +/- 0.1  | 1.1 +/- 0.08 | 1.1 +/- 0.07 | 0.8 +/- 0.1  | 0.5 +/- 0.06  |
| LOVO   | DMSO | 1.5 +/- 0.06       | 1.6 +/- 0.06     | 0.06 +/- 0.003        | 0.6 +/- 0.08   | 0.3 +/- 0.03 | 0.7 +/- 0.1  | 2.4 +/- 0.3  | 16.3 +/- 1.1 | 1.4 +/- 0.3   |
|        | DAPT | 2.8 +/- 0.02       | 0.9 +/- 0.09     | 0.2 +/- 0.02          | 0.8 +/- 0.01   | 0.5 +/- 0.02 | 0.9 +/- 0.03 | 1.6 +/- 0.2  | 9.6 +/- 0.6  | 1.9 +/- 0.2   |
| RKO    | DMSO | 0.0009 +/- 0.0001  | 0.03 +/- 0.002   | 0.000006 +/- 0.000004 | 2.0 +/- 0.2    | 0.1 +/- 0.02 | 0.7 +/- 0.04 | 1.4 +/- 0.3  | 0.3 +/- 0.03 | 1.3 +/- 0.3   |
|        | DAPT | 0.0004 +/- 0.00003 | 0.002 +/- 0.0005 | 0.000006 +/- 0.000001 | 2.3 +/- 0.1    | 0.2 +/- 0.02 | 1.3 +/- 0.05 | 1.2 +/- 0.09 | 0.4 +/- 0.06 | 2.4 +/- 0.3   |
| SW480  | DMSO | 0.001 +/- 0.0001   | 0.07 +/- 0.02    | 0.00005 +/- 0.000004  | 0.02 +/- 0.006 | 0.3 +/- 0.06 | 0.7 +/- 0.1  | 2.4 +/- 0.3  | 1.2 +/- 0.3  | 1.3 +/- 0.3   |
|        | DAPT | 0.001 +/- 0.0001   | 0.04 +/- 0.006   | 0.00004 +/- 0.00001   | 0.03 +/- 0.007 | 0.3 +/- 0.06 | 0.8 +/- 0.08 | 1.6 +/- 0.2  | 1.6 +/- 0.3  | 1.9 +/- 0.3   |
| HCT116 | DMSO | 0.001 +/- 0.0002   | 0.7 +/- 0.06     | 0.00002 +/- 0.000006  | 0.4 +/- 0.06   | 0.2 +/- 0.03 | 0.5 +/- 0.02 | 1.7 +/- 0.8  | 5.7 +/- 0.4  | 0.9 +/- 0.1   |
|        | DAPT | 0.002 +/- 0.0002   | 0.5 +/- 0.05     | 0.00005 +/- 0.00002   | 0.3 +/- 0.02   | 0.2 +/- 0.03 | 0.5 +/- 0.1  | 1.2 +/- 0.1  | 4.6 +/- 0.3  | 1.5 +/- 0.1   |